Study on the photonic bandgaps of hollow-core microstructured fibers

Zhaolun Liu (刘兆伦), Guiyao Zhou (周桂耀), and Lantian Hou (侯蓝田)

Institute of Infrared Optical Fibers and Sensors, Yanshan University, Qinhuangdao 066004

Received April 5, 2006

A simple method is presented to measure the transmission spectrum of hollow-core microstructured fibers in the visible, near-infrared, and mid-infrared regions. The plane wave expansion method is applied to analyze the photonic bandgaps of hollow-core microstructured fibers. The experimental results indicate that there are several strong transmission bands in the near-infrared and mid-infrared region, but hardly any transmission phenomena in the visible region, which shows that there are some bandgaps in near-infrared wavelength. The experimental results are consistent with the numerically simulative results using a plane wave expansion method.

OCIS codes: 060.2270, 060.2300, 060.2400.

Microstructured fibers (MFs), also called photonic crystal fibers (PCFs) which are characterized by a periodic arrangement of air holes around the core along the entire length of the fiber, have attracted much interest in telecommunication and sensing[1,2]. MFs have flexibility of design and can achieve many extraordinary characteristics, such as single mode guidance over a wide spectral range, high nonlinearity, photonic bandgap (PBG) guidance, and others[3−5]. For hollow-core microstructured fibers (HC-MFs), the guidance mechanism is photonic bandgap effect guidance[2,6].

Figure 1 is the scanning electron microscope (SEM) image of HC-MFs we used. The structure parameters of HC-MFs: the radius of the centric air hole is 3.75 μm, the pitch Λ is 2.65 μm, the air-hole diameter d of the cladding is 2.10 μm, and the air filling rate f of the cladding is about 52%. We propose to simulate the photonic bandgaps of HC-MFs using a numerical method and measure the transmission spectrum of HC-MFs.

Numerical simulations play an important role for the design and modeling of MFs. So far, various modeling methods such as effective index approach, plane-wave expansion (PWE) method, localized-function method, multipole method, and finite-element method (FEM) have been developed[7−12]. However, whereas scalar versions of these methods may be sufficient for modeling specific cases of effective-index guiding MFs, modeling of true PBG guiding fibers requires full-vectorial methods[8,9]. We employ PWE method for solving the vectorial magnetic field wave equation as an eigenvalue problem.

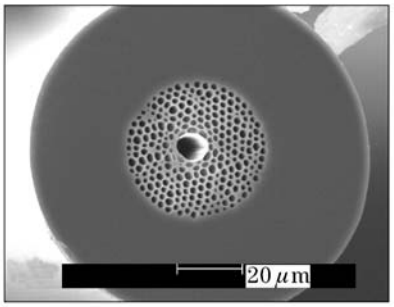

Fig. 1. SEM image of HC-MFs.

The PWE method can be applied to compute the PBGs of photonic crystal and MF[10−12]. The Maxwell's equations in a transparent, time-invariant, source free and non-permeable space can be rewritten as Helmholz's equations[9]:

$$\nabla \times \nabla \times \overrightarrow{E}(\overrightarrow{r}) = \frac{\omega^2}{c^2}\varepsilon(r)\overrightarrow{E}(\overrightarrow{r}), \tag{1}$$

$$\nabla \times \left[\frac{1}{\varepsilon(r)}\nabla \times \overrightarrow{H}(\overrightarrow{r})\right] = \frac{\omega^2}{c^2}\overrightarrow{H}(\overrightarrow{r}), \tag{2}$$

where $\overrightarrow{E}$ is electric field, $\overrightarrow{H}$ is magnetic field. $\varepsilon(r)$ is the waveguide dielectric function, ω is the angular frequency, and c is the speed of light in vacuum.

In an infinite periodic photonic crystal, using Bloch's theorem, a mode in a periodic structure can be expanded as a sum of infinite number of plane waves[9]:

$$\vec{H}(r) = \hat{e}_k \mathrm{e}^{i\vec{k}\cdot\vec{r}} \sum_{G_i} h(G_i)\mathrm{e}^{i\overrightarrow{G}\cdot\vec{r}}$$

$$= \sum_{G_i,\lambda} h(G_i,\lambda)\mathrm{e}^{i(\vec{k}+\overrightarrow{G}_i)\cdot\vec{r}}\hat{e}_{\lambda,\vec{k}+\overrightarrow{G}_i}, \tag{3}$$

where $\lambda = 1, 2$, $\vec{k}$ is the wave vector of the plane wave, $\overrightarrow{G}$ is the reciprocal lattice vector, $\hat{e}_{\lambda,\vec{k}+\overrightarrow{G}_i}$ is the unit vector perpendicular to $\vec{k}+\overrightarrow{G}$, and $h(G_i,\lambda)$ is the component amplitude along the unit vector.

Using the Fourier transform, Helmholz's equations can be transformed to an algebraic form[9]:

$$\sum_{\overrightarrow{G}} \left|\overrightarrow{k}+\overrightarrow{G}\right| \left|\overrightarrow{k}+\overrightarrow{G}'\right| \varepsilon^{-1}(\overrightarrow{G}-\overrightarrow{G}')$$

$$\times \begin{bmatrix} \hat{e}_2\cdot\hat{e}_2' & -\hat{e}_2\cdot\hat{e}_1' \\ -\hat{e}_1\cdot\hat{e}_2' & \hat{e}_1\cdot\hat{e}_1' \end{bmatrix} \begin{bmatrix} h_1' \\ h_2' \end{bmatrix} = \frac{\omega^2}{c^2} \begin{bmatrix} h_1 \\ h_2 \end{bmatrix}. \tag{4}$$

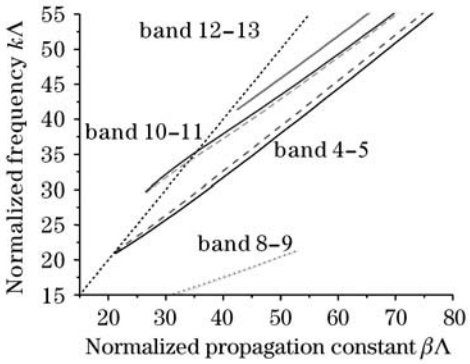

Fig. 2. Simulated photonic bandgaps image of HC-MFs.

Figure 2 shows the computed PBGs image of HC-MFs using PWE method, we can see there are four obvious PBGs, that is, band 4—5, band 8—9, band 10—11, and band 12—13 respectively.

On the basis of the theoretical study on PBG of HC-MFs, it is necessary to demonstrate the positions of the PBG using experimental analyses. We know light cannot propagate from the cladding when the frequency falls in the PBG. According to this, we measured the transmission spectrum of HC-MFs to analyze the PBGs of HC-MFs.

To measure the transmission spectrum of HC-MFs we need special preparation of the samples because we have used the samples without outer cladding. The experimental setup used for the following measurements is shown in Fig. 3, which includes the following parts: light source, monochromator, spectrometer, detector, coupler, HC-MFs sample, etc.. The sample of the measured fiber is 13 cm long. To insure the light intensity, light source should aim at the surface of the fiber accurately, thus there requiring a coupler equipment. Light signal is sent to the fiber, through the detector and the lock-in amplifier, and then collected by the data acquisition, we can obtain the curve between the light energy and wavelength on the computer. The modulating disk in this system is the device which can modulate light periodically. It transfers the DC signal to the AC signal. To insure the precision of the measurement, the AC signal as the referenced signal is sent to the lock-in amplifier, and then the light signal out of the tested fibers is locked, which can conquer the influence of the direct current excursion and dim-current.

Figures 4 and 5 show the experimental results for the transmission spectra of the visible region and infrared region respectively. From Fig. 4, we can see that there

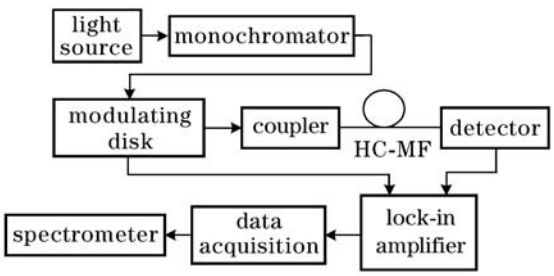

Fig. 3. Experimental setup for transmission spectrum measurements.

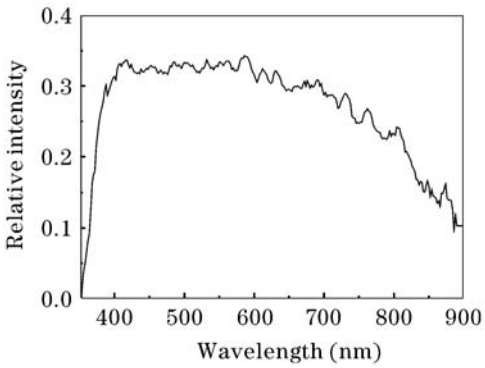

Fig. 4. Transmission spectrum for visible region.

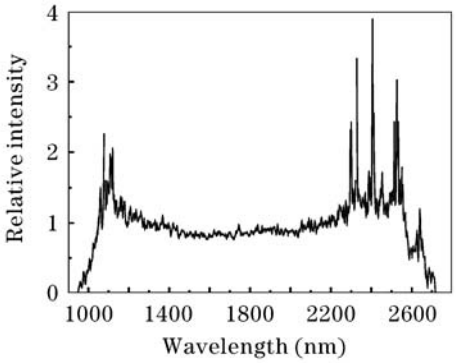

Fig. 5. Transmission spectrum for near-infrared and mid-infrared region.

are no distinct transmission phenomena; from Fig. 5, we find that there are several strong transmission bands in the near-infrared region and mid-infrared region, the positions are at 1108, 2297, 2406, and 2525 nm respectively. The experimental results are consistent with the calculation results using PWE method.

In conclusion, we computed the PBGs of HC-MFs using PWE method, and measured the transmission spectrum of HC-MFs in the visible, near-infrared and mid-infrared regions utilizing transmission spectrum method to analyze the PBGs of HC-MFs. The experimental results show that there are three bandgaps which occur at the near-infrared region and mid-infrared region, which are consistent with the calculation results. We measured HC-MFs repeatedly, and the repetition of the experiment is well, which demonstrates the feasibility of the method. The results can offer the base for the fabrication and application of HC-MFs.

This work was supported by the National High Technology Development Program of China (No. 2003AA311010), and the National Key Basic Research and Development Program of China (No. 2003CB314905). Z. Liu's e-mail address is lhx_zl@163.com.

References

1. P. Russell, Science **299,** 358 (2003).
2. D. G. Ouzounov, F. R. Ahmad, D. Müller, N. Venkataraman, M. T. Gallagher, M. G. Thomas, J. Silcox, K. W. Koch, and A. L. Gaeta, Science **301,** 1702 (2003).

3. M. Yan and P. Shum, IEEE Photon. Technol. Lett. **17,** 64 (2005).
4. M. Yan, P. Shum, and J. Hu, Opt. Lett. **30,** 465 (2005).
5. A. Zhang and M. S. Demokan, Opt. Lett. **30,** 2375 (2005).
6. J. Lægsgaard, Opt. Lett. **30,** 3281 (2005).
7. K. Saiton and M. Koshiba, J. Lightwave Technol. **23,** 3580 (2005).
8. L. Vincetti, F. Poli, and S. Selleri, IEEE Photon. Technol. Lett. **18,** 508 (2006).
9. S. Guo and S. Albin, Opt. Express **11,** 167 (2003).
10. M. Chen and R. Yu, IEEE Photon. Technol. Lett. **16,** 819 (2004).
11. Y. Li, C. Wang, M. Hu, B. Liu, X. Sun, and L. Chai, Opt. Express **13,** 6856 (2005).
12. Y. Li, C. Wang, M. Hu, B. Liu, X. Sun, and L. Chai, IEEE Photon. Technol. Lett. **18,** 262 (2006).